

The Selective Cause of an Ancient Adaptation

Guoping Zhu,^{1*} G. Brian Golding,³ Antony M. Dean^{1,2,†}

Phylogenetic analysis reveals that the use of nicotinamide adenine dinucleotide phosphate (NADP) by prokaryotic isocitrate dehydrogenase (IDH) arose around the time eukaryotic mitochondria first appeared, about 3.5 billion years ago. We replaced the wild-type gene that encodes the NADP-dependent IDH of *Escherichia coli* with an engineered gene that possesses the ancestral NAD-dependent phenotype. The engineered enzyme is disfavored during competition for acetate. The selection intensifies in genetic backgrounds where other sources of reduced NADP have been removed. A survey of sequenced prokaryotic genomes reveals that those genomes that encode isocitrate lyase, which is essential for growth on acetate, always have an NADP-dependent IDH. Those with only an NAD-dependent IDH never have isocitrate lyase. Hence, the NADP dependence of prokaryotic IDH is an ancient adaptation to anabolic demand for reduced NADP during growth on acetate.

A central goal in evolutionary biology is the understanding of the mechanisms underlying ancient adaptive events (1). Guided by phylogenetic analysis, genetic engineering has been used to reconstruct ancestral genes, allowing ancient phenotypes to be revealed (2–5). Reconstruction can tell us what the ancestral phenotype was like, but it does not tell us why the modern phenotype evolved. Were the changes adaptive or just due to chance? If they were adaptive, what was the basis of that adaptation? Rigorous tests of hypotheses regarding adaptation are needed to identify the mutations responsible for changes in function and to demonstrate that they are selectively advantageous under the conditions specified (6). This has yet to be achieved for any reconstructed gene. The isocitrate dehydrogenase (IDH) system offers an opportunity to elucidate the adaptive basis of an ancient functional change.

Phylogenetics. IDHs belong to a large, ubiquitous, and very ancient family of enzymes that play central roles in energy metabolism (7, 8), amino acid biosynthesis (9, 10), and vitamin production (11). Although most family members use nicotinamide adenine dinucleotide (NAD) to oxidize their substrates, some IDHs, including that of *E. coli*, use NADP instead (7).

¹BioTechnology Institute, ²Department of Ecology, Evolution, and Behavior, University of Minnesota, St. Paul, MN 55108, USA. ³Department of Biology, McMaster University, Hamilton, Ontario L8S 4K1, Canada.

*Present address: Department of Biology, Anhui Normal University, Wuhu 241000, People's Republic of China.

†To whom correspondence should be addressed. E-mail: adean@biosci.umn.edu

Phylogenetic analyses reveal that NAD use is an ancestral trait and that NADP use by prokaryotic IDH arose on or about the time that eukaryotic mitochondria first appeared,

some 3.5 billion years ago (Fig. 1). Phylogenetic trees were constructed using maximum parsimony and neighbor joining, with deep branches swapped and assessed by maximum likelihood (12). Different phylogenetic methods often give slightly different trees, and others produce sets of slightly different trees whose likelihoods are indistinguishable. This is especially true when considering deep phylogenies whose sequences diverged from a common ancestor billions of years ago. For the ancient family of IDHs and isopropylmalate dehydrogenases (IMDHs), short branches among the deeper nodes lead to a large number of trees with similar likelihoods. Nevertheless, all trees contain three well-supported monophyletic groups: type I IDHs, the highly divergent type II IDHs, and the NAD-IMDHs and related enzymes. There is no suitable outgroup. Instead, we rooted the phylogeny on the branch linking the IDHs to the IMDHs because the common ancestor was undoubtedly prototrophic, capable of synthesizing glutamate and leucine, and hence must have had both enzymatic functions (13). This root implies that specificity toward NADP

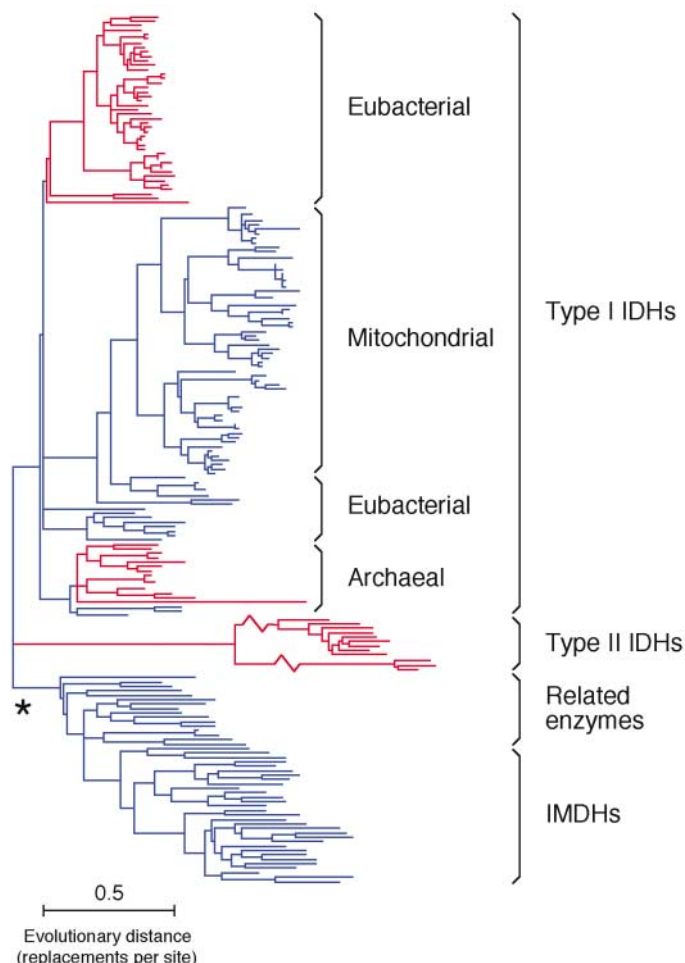


Fig. 1. A maximum likelihood phylogeny of the IDH family. This tree, like all others with similar likelihoods, reveals that NADP use evolved independently several times (red lineages) billions of years ago, around the time eukaryotic mitochondria first appeared. The asterisk represents the approximate position of the root based on biochemical evidence (13).

arose in prokaryotes several times, on or about the time the eukaryotic mitochondria first appeared, some 3.5 billion years ago.

Recent structural comparisons (14) confirm that NADP use by type I IDHs evolved independently from the use of NADP by type II IDHs and that the monomeric type II IDHs (lower cluster, eubacterial) are derived from the dimeric enzymes (upper cluster, eubacterial and eukaryotic). Specificity toward NADP may have arisen twice within the type I IDHs, because the same suite of amino acid replacements for binding NADP are found in both the eubacterial and archaeal lineages. Other trees with similar likelihoods lead to similar conclusions. We conclude that the use of NADP is an ancient adaptation that arose on at least three occasions in early prokaryotes.

Structural biology. To identify the amino acids that are responsible for the change in specificity from NAD to NADP, it would be ideal to compare the structures of NADP-using with NAD-using IDHs and contrast the modes of coenzyme binding. Unfortunately, no such structures of NAD-using IDHs are available. Although divergent in sequence, IMDHs are homologous to the IDHs (Fig. 1) and structurally very similar to the IDHs, and they use NAD (Fig. 2A). Amino acid residues determining coenzyme use were identified from high-resolution crystallographic structures of the binary complexes of NADP bound to *E. coli* IDH (15) and of NAD bound to *Thermus thermophilus* IMDH (16) (Fig. 2A). Maximum likelihood reconstruction of ancestral sequences confirmed that all six conserved residues binding NADP in prokaryotic IDHs were introduced in very ancient times (13). This analysis also revealed that the three key residues conferring specificity toward NAD are ancestral and that the others are not conserved in NAD-specific family members, because they have no role in binding NAD.

Protein engineering. Protein engineering (Fig. 2B) was used to switch the coenzyme specificity of *E. coli* IDHs from NADP to NAD (17). That experiment showed that amino acids in the active site, and no others, determine specificity. Our engineered IDH has five replacements in the active site. Three [Lys344Asp (where Lys³⁴⁴ is replaced by Asp), Tyr345Ile, and Val351Ala] are conserved, ancestral, and confer specificity toward NAD, and two (Tyr391Lys and Arg395Ser) are not conserved and simply remove interactions with the 2'-phosphate of NADP. The engineered IDH has two additional replacements (Cys201Met and Cys332Tyr) outside the active site that increase overall activity but do not affect specificity. X-ray crystallography (Fig. 2B) shows that the engineered IDH binds NAD in precisely the same manner as wild-type IMDH (18). Kinetic studies (17) show that specificity was inverted by a factor of 1.4 million, from a 7000-fold preference for NADP ($k_{\text{cat}}^{\text{NADP}}/K_{\text{m}}^{\text{NADP}} = 4.7 \times 10^6 \text{ M}^{-1} \text{ s}^{-1}$, $k_{\text{cat}}^{\text{NAD}}/K_{\text{m}}^{\text{NAD}} = 690 \text{ M}^{-1} \text{ s}^{-1}$, where k_{cat} is the catalytic rate constant and K_{m} is the Michaelis constant) to a 200-fold preference for NAD ($k_{\text{cat}}^{\text{NADP}}/K_{\text{m}}^{\text{NADP}} = 810 \text{ M}^{-1} \text{ s}^{-1}$, $k_{\text{cat}}^{\text{NAD}}/K_{\text{m}}^{\text{NAD}} = 1.64 \times 10^5 \text{ M}^{-1} \text{ s}^{-1}$). With a $k_{\text{cat}} = 16.2 \text{ s}^{-1}$ and a $K_{\text{m}} = 99 \text{ }\mu\text{M}$, our engineered IDH is as active as naturally occurring NAD-dependent members of the family (17).

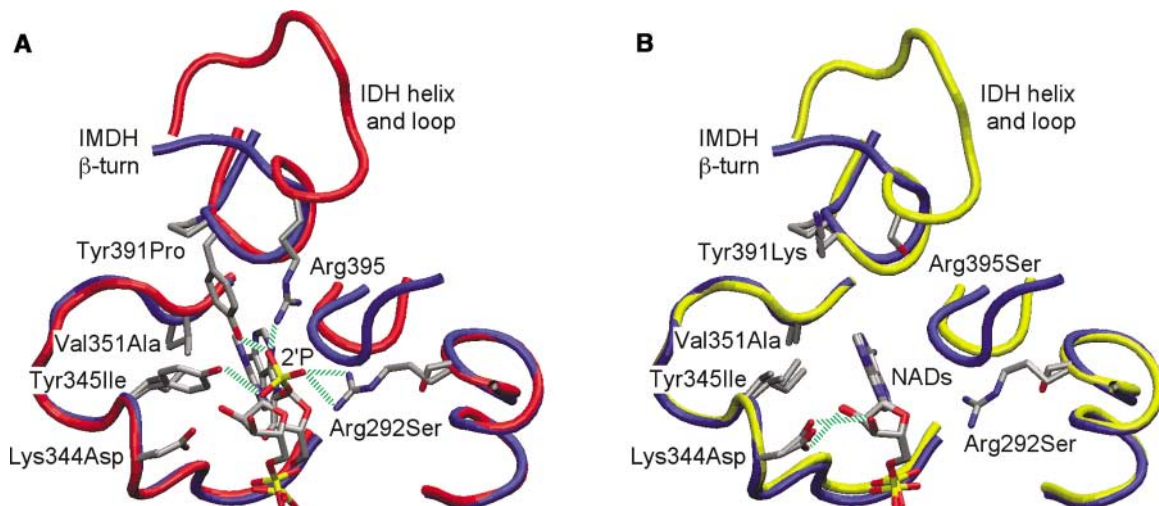
Metabolism. Previously (13), we hypothesized that the use of NADP by prokaryotic IDHs is an adaptation to growth on acetate. When bacteria grow on highly reduced (energy-rich) compounds such as glucose, NADPH (the reduced form of NADP) for biosynthesis is obtained by diverting energy-rich carbon from glycolysis into the oxidative branch of the pentose phosphate pathway (19). During growth on acetate, which is a highly oxidized (energy-poor) compound, there is no energy-rich carbon to divert into the oxidative branch,

and therefore alternative sources of NADPH are required. These are a transhydrogenase (PntAB) encoded by the gene *pntAB* (20), an NADP-dependent malic enzyme (MAEB) encoded by *maeB* (21), and the NADP-dependent IDH encoded by *icd* (22). Metabolic flux analyses of *E. coli* consuming acetate show that IDH provides about 90% of the NADPH (21, 23–25).

Competition studies. Testing whether the use of NADP by eubacterial type I IDH is an adaptation to growth on acetate requires competing strains that differ only at their chromosomally located *icd* gene. Therefore, the wild-type chromosomal copy of *icd*^{NADP} was replaced with the engineered *icd*^{NAD} (26). Chemostat competition experiments (27–29) were conducted in a minimal salts medium with either acetate or glucose as the sole limiting nutrient. The engineered *icd*^{NAD} was strongly selected against during competition for acetate, yet favored slightly over wild-type *icd*^{NADP} during competition for glucose (Fig. 3). These results support our hypothesis that the switch in coenzyme specificity by IDH was driven by the need to supply additional NADPH for biosynthesis during growth on acetate.

Cause of selection. The selection on acetate might be attributed to the engineered IDH having altered kinetic characteristics toward isocitrate and/or being less efficiently regulated by IDH kinase/phosphatase (30), rather than attributed to the switch in coenzyme use. We reasoned that the selection at *icd*, if caused by the change in coenzyme use, should intensify as other sources of NADPH are removed (MAEB and PntAB), because IDH would now contribute proportionally more reducing power to biosynthesis. By contrast, selection at *icd* is not expected to intensify if the change in coenzyme use is of no functional consequence.

Fig. 2. Structural analysis reveals the modes of binding of NADP and NAD in the active sites of IDH and IMDH. Only key residues are shown, with side chains colored using the CPK (Corey, Pauling, and Koltun) convention (gray, carbon; red, oxygen; blue, nitrogen; yellow, phosphorus). Labels designate the IDH amino acid, the site number in *E. coli* IDH, and the IMDH amino acid. (A) Wild-type *E. coli* IDH (main chain red) with H bonds (green dashes) to the 2'-phosphate of NADP (2'P) superimposed on wild-type *T. thermophilus* IMDH (main chain blue) with NAD. (B) Engineered IDH (main chain yellow) reveals that NAD binds in precisely the same manner as seen in *T. thermophilus* IMDH and that the same H bonds form to the ribose hydroxyls.



Strains with deletions of *maeB*, *pntAB*, and *udhA* (which encodes a soluble transhydrogenase, UdhA) that are generated by the method of Datsenko and Wanner (31) grow so slowly on acetate relative to the wild type (most simply wash out from the chemostat) that fitnesses were best estimated from growth rates in batch cultures (26). Table 1 presents the growth rates of the engineered *icd*^{NAD} relative to *icd*^{NADP} in various genetic backgrounds. On acetate, selection against the engineered *icd*^{NAD} in $\Delta pntAB$ and $\Delta maeB$ backgrounds intensifies as the number of NADPH-producing steps declines. Selection against the engineered *icd*^{NAD} is much weaker in the control experiments on glucose because other pathways provide the bulk of NADPH for growth.

In $\Delta udhA$ backgrounds, the engineered *icd*^{NAD} can be favored over the wild-type allele (Table 1). UdhA is a soluble transhydrogenase that, unlike PntAB, lacks a source of energy to drive hydride transfer from one coenzyme to another (25). Consequently, the overall direction of the UdhA-catalyzed reaction depends on the ratios of NADH to NAD and of NADPH to NADP. In wild-type cells growing on acetate, UdhA usually favors production of NADH through the oxidation (or reoxidation) of abundant

NADPH (25). Replacing *icd*^{NADP} with the engineered *icd*^{NAD} in a $\Delta udhA$ genetic background increases NADH production and improves fitness (Table 1). Deleting *pntAB* and/or *maeB* does nothing to restore NADH levels, and fitness does not improve (32). These results confirm that UdhA is an important source of NADH during growth on acetate, but not on glucose (Table 1). These experiments demonstrate that the engineered *icd*^{NAD} can provide NADH for energy in certain mutant genetic backgrounds.

These results are entirely in accord with the hypothesis that selection on acetate is caused by the change in coenzyme use and not by changes in kinetics toward isocitrate and/or changes in regulatory phosphorylation. We speculate that evolutionary functional reversals at *icd* might be possible if NADH production becomes limited (if adaptive changes in other steps reduce NADH production as a correlated response) or if demand for NADH increases because of some environmental change (for example, growth at an extreme ionic strength or extraction of scarce resources from the environment, either of which can make increased energetic demands on membrane transporters).

Genomic comparisons. Complete genome sequences provide additional support

for our hypothesis. Isocitrate lyase (ICL) is essential for growth on acetate and provides carbon for biosynthesis by diverting isocitrate into the glyoxylate bypass and away from the two CO₂-releasing steps in the Krebs cycle (7, 19, 21, 23–25). Without exception, each of the 46 prokaryotic genomes encoding an ICL has an NADP-dependent IDH, and no ICL is found in the 12 genomes encoding an NAD-dependent IDH (table S1). Although shared phylogenetic histories contribute to this pattern (for example, four species of *Bacillus* have ICLs and NADP-dependent IDHs and two species of *Rickettsia* have only NAD-dependent IDHs), they do not explain it. Members of both groups are highly diverse and include archaea, bacilli, and α - and γ -proteobacteria. Moreover, within each group are species with varied metabolic life-styles from diverse habitats. Each contains auto-, hetero-, chemo-, and lithotrophs; intra- and extracellular parasites; and organisms isolated from environments that vary from aerobic to anaerobic, from temperate to extremely hot, and from acidic to basic (33). Because the tight association between ICL and use of NADP by IDH is independent of taxonomic group, metabolic life-style, and physical habitat, we argue that the benefit to IDH of using NADP during growth on acetate is general and not particular to our experiments.

Conclusions. Was the switch in specificity from NAD to NADP by IDH adaptive or due to chance? The finding that the use of NAD arose on at least three independent occasions argues that the switch was adaptive. What was the basis of that adaptive switch? Physiological analysis using an *E. coli* IDH engineered to use NAD shows that use of NADP is strongly favored during growth on acetate. The 4% increase in growth rate in batch culture is a huge selective advantage that could produce a >50-fold increase in the ratio of *icd*^{NADP} to *icd*^{NAD} within just 100 generations. The 9% increase seen when *E. coli* strains were starved in chemostats could produce a >8000-fold enrichment within the same number of generations. Because all 46 prokaryotes with the ICL essential for growth on acetate also have an NADP-dependent IDH, and all 12 prokaryotes with only an NAD-dependent IDH have no ICL, the selection on acetate is not a laboratory artifact. Instead, it represents an adaptation to acetate use; one that was very likely the basis for the ancient recurrent switch to use of NADP by IDH.

We have shown that it is possible to reconstruct not only what occurred (the switch to NADP use by IDH) in an ancient adaptive event and how it occurred (changes at five specific amino acids in IDH), but also why it occurred (adaptation to growth on acetate or other similar energy-poor resources). Our studies provide a general approach to the reconstruction of ancient adaptive events.

Fig. 3. Chemostat competition experiments. The slopes of the lines, *s*, are estimated selection coefficients per generation. The engineered *icd*^{NAD} is much less fit than the wild-type *icd*^{NADP} on acetate (solid circle), yet fitter on glucose (open circles). Presented are the pooled results from three chemostat competitions on each carbon source.

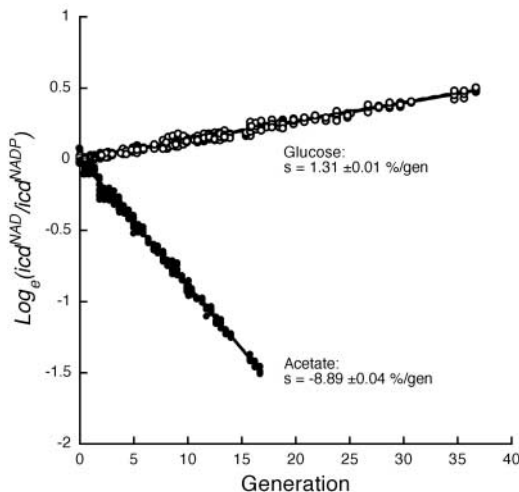


Table 1. Growth rates of *icd*^{NAD} relative to *icd*^{NADP} in various genetic backgrounds.

Genetic background	Relative growth rate (<i>icd</i> ^{NAD} / <i>icd</i> ^{NADP})*	
	Acetate	Glucose
Wild type	0.96 ± 0.02	0.998 ± 0.008
$\Delta pntAB$	0.73 ± 0.04	0.991 ± 0.007
$\Delta maeB$	0.63 ± 0.04	0.991 ± 0.006
$\Delta pntAB, \Delta maeB$	0.44 ± 0.03	0.963 ± 0.008
$\Delta udhA$	1.46 ± 0.03	0.990 ± 0.004
$\Delta udhA, \Delta pntAB$	1.65 ± 0.09	0.992 ± 0.005
$\Delta udhA, \Delta maeB$	0.95 ± 0.11	0.975 ± 0.003
$\Delta udhA, \Delta pntAB, \Delta maeB$	0.16 ± 0.05	0.974 ± 0.003

*Growth rates were determined in minimal medium with either acetate or glucose as the sole source of carbon and energy.

Phylogenetics provides molecular history. Structural biology reveals key replacements that are responsible for functional changes. Protein engineering tests the relationships between form and function. Studies of metabolism (physiology, development, and behavior in higher organisms) identify selectable phenotypes. Competition studies provide a means to explore the adaptive basis of any claim. Genomic comparisons confirm the generality of the results. By completing each of these steps, it is possible to identify the most probable cause of an ancient adaptive event that occurred billions of years ago.

References and Notes

- G. B. Golding, A. M. Dean, *Mol. Biol. Evol.* **15**, 355 (1998).
- T. M. Jermann, J. G. Opitz, J. Stackhouse, S. A. Benner, *Nature* **374**, 57 (1995).
- J. Zhang, Y. P. Zhang, H. F. Rosenberg, *Nature Genet.* **30**, 411 (2002).
- E. A. Gaucher, J. M. Thomson, M. F. Burgan, S. A. Benner, *Nature* **425**, 285 (2003).
- Y. Shi, S. Yokoyama, *Proc. Natl. Acad. Sci. U.S.A.* **100**, 8308 (2003).
- B. Clarke, *Genetics* **79** (suppl.), 101 (1975).
- D. Voet, J. G. Voet, *Biochemistry* (Wiley, New York, 1995).
- P. A. Tipton, B. S. Beecher, *Arch. Biochem. Biophys.* **313**, 15 (1994).
- H. Kirino, T. Oshima, *J. Biochem.* **109**, 852 (1991).
- J. Miyazaki, N. Kobashi, M. Nishiyama, H. Yamane, *J. Biol. Chem.* **278**, 1864 (2003).
- J. Sivaraman *et al.*, *J. Biol. Chem.* **278**, 43682 (2003).
- J. Felsenstein, PHYLIP ver. 3.5 (Univ. of Washington, Seattle, WA, 1994).
- A. M. Dean, G. B. Golding, *Proc. Natl. Acad. Sci. U.S.A.* **94**, 3104 (1997).
- Y. Yasutake *et al.*, *J. Biol. Chem.* **278**, 36897 (2003).
- J. H. Hurley, A. M. Dean, D. E. Koshland Jr., R. M. Stroud, *Biochemistry* **30**, 8671 (1991).
- J. H. Hurley, A. M. Dean, *Structure* **2**, 1007 (1994).
- R. Chen, A. Greer, A. M. Dean, *Proc. Natl. Acad. Sci. U.S.A.* **92**, 11666 (1995).
- J. H. Hurley, R. Chen, A. M. Dean, *Biochemistry* **35**, 5670 (1996).
- F. C. Neidhardt, J. L. Ingraham, M. Schaechter, *Physiology of the Bacterial Cell: A Molecular Approach* (Sinauer, Sunderland, MA, 1990).
- D. M. Clarke, T. W. Loo, S. Gillam, P. D. Bragg, *Eur. J. Biochem.* **158**, 647 (1986).
- J. Zhao, K. Shimizu, *J. Biotechnol.* **101**, 101 (2003).
- P. E. Thorsness, D. E. Koshland Jr., *J. Biol. Chem.* **262**, 10422 (1987).
- K. Walsh, D. E. Koshland Jr., *J. Biol. Chem.* **259**, 9646 (1984).
- K. Walsh, D. E. Koshland Jr., *J. Biol. Chem.* **260**, 8430 (1985).
- U. Sauer, F. Canonaco, S. Heri, A. Perrenoud, E. Fischer, *J. Biol. Chem.* **279**, 6613 (2004).
- Materials and methods are available as supporting material on Science Online.
- D. E. Dykhuizen, *Methods Enzymol.* **224**, 613 (1993).
- M. Lunzer, A. Natarajan, D. E. Dykhuizen, A. M. Dean, *Genetics* **162**, 485 (2002).
- A. M. Suiter, O. Bänzinger, A. M. Dean, *Proc. Natl. Acad. Sci. U.S.A.* **100**, 12782 (2003).
- S. P. Miller *et al.*, *J. Biol. Chem.* **275**, 833 (2000).
- K. A. Datsenko, B. L. Wanner, *Proc. Natl. Acad. Sci. U.S.A.* **97**, 6640 (2000).
- G. Zhu, G. B. Golding, A. M. Dean, unpublished data.
- M. T. Madigan, J. M. Martinko, J. Parker, *Brock Biology of Microorganisms* (Prentice-Hall, Upper Saddle River, NJ, ed. 9, 2000).
- We thank M. Lunzer and S. Miller for technical assistance and B. Hall, B. Kerr, L. Merlo, S. Miller, and R. Redfield for constructive criticism of the manuscript. Supported by NIH grant GM060611 (A.M.D.).

1 November 2004; accepted 14 December 2004

Published online 13 January 2005;

10.1126/science.1106974

Include this information when citing this paper.

Axonopathy and Transport Deficits Early in the Pathogenesis of Alzheimer's Disease

Gorazd B. Stokin,¹ Concepción Lillo,² Tomás L. Falzone,¹ Richard G. Brush,¹ Edward Rockenstein,³ Stephanie L. Mount,¹ Rema Raman,⁵ Peter Davies,⁶ Eliezer Masliah,^{3,4} David S. Williams,^{2,3} Lawrence S. B. Goldstein^{1*}

We identified axonal defects in mouse models of Alzheimer's disease that preceded known disease-related pathology by more than a year; we observed similar axonal defects in the early stages of Alzheimer's disease in humans. Axonal defects consisted of swellings that accumulated abnormal amounts of microtubule-associated and molecular motor proteins, organelles, and vesicles. Impairing axonal transport by reducing the dosage of a kinesin molecular motor protein enhanced the frequency of axonal defects and increased amyloid- β peptide levels and amyloid deposition. Reductions in microtubule-dependent transport may stimulate proteolytic processing of β -amyloid precursor protein, resulting in the development of senile plaques and Alzheimer's disease.

Axons and axonal transport exhibit prominent defects in a wide variety of neurological diseases. These defects often manifest as axonal swellings or spheroids, which correspond to axonal enlargements and aberrant accumula-

tions of axonal cargos and cytoskeletal proteins (1). Molecular motor proteins propel axonal cargoes to and from presynaptic terminals along microtubule tracks and are thus crucial to understanding the role of impaired axonal transport in the pathogenesis of neurological diseases. A number of observations suggest that axonal transport may fail during the progression of Alzheimer's disease (AD) (2). We tested for axonal defects that are diagnostic of transport deficits and that might be related to early stages in the pathogenesis of AD.

AD is a common neurodegenerative disorder characterized by progressive cognitive deterioration and severe synaptic and neuronal

loss. Pathological hallmarks of this disease—neurofibrillary tangles, neuropil threads, and senile plaques—are potentially linked to alterations of the axonal compartment (3). Neurofibrillary tangles and neuropil threads are related to the abnormal phosphorylation of the microtubule-associated protein tau and its dislocation from axons to presynaptic terminals and somatodendritic compartments. Senile plaques are composed of dystrophic neurites, some but not all of which are embedded in a matrix of extracellular amyloid. Some dystrophic neurites correspond to axonal swellings, which often contain abnormal accumulations of axonal cargos and tau (4).

Familial AD (FAD) mutations in β -amyloid precursor protein (β APP) and in presenilin genes (PS1 and PS2) alter the production of amyloid- β peptides (A β s), the major constituents of senile plaques, suggesting that proteolytic processing of β APP into A β s plays a central role in AD pathogenesis (5). In neurons, β APP and its proteolytic machinery, PS1 and β -site β APP cleaving enzyme (BACE), undergo kinesin-I-mediated fast anterograde axonal transport (6–9), during which β APP may undergo proteolysis into A β -bearing intermediates (10) and A β s (7, 11). Increased A β levels (11, 12) and senile plaques (13, 14) in the axon-enriched white matter of mouse model and human AD brains suggest aberrant A β generation, or degradation, in axons. Reduced brain white matter in β APP-deficient mice (15) also indicates that β APP plays a role in axonal structure and function. Similar phenotypes have been found in a mouse model of AD (16) and in human AD (17), suggesting that axonal failure is an important part of AD. Overexpression of β APP in *Drosophila* causes axonal transport defects, which are markedly enhanced by ordinarily

¹Howard Hughes Medical Institute and Department of Cellular and Molecular Medicine, ²Department of Pharmacology, ³Department of Neurosciences, ⁴Department of Pathology, ⁵Department of Family and Preventive Medicine, School of Medicine, University of California San Diego (UCSD), 9500 Gilman Drive, La Jolla, CA 92093, USA. ⁶Department of Pathology, F526, Albert Einstein College of Medicine, 1300 Morris Park Avenue, New York, NY 10461, USA.

*To whom correspondence should be addressed. E-mail: lgoldstein@ucsd.edu